Table 4.10: Daily precipitation in inches at Hopi as reported by the NOAA Grand Canyon weather monitoring station.

Jan 1	t	Feb 1	.01
Jan 2	t	Feb 4	.18
Jan 3	t	Feb 10	.09
Jan 4	t	Feb 11	.06
Jan 5	.35	Feb 12	.14
Jan 6	.16	Feb 14	.22
Jan 7	.05	Feb 16	t
Jan 8	.07	Feb 17	t
Jan 16	.03		
Jan 17	.02		
Jan 20	.08		
Jan 28	t		
Jan 29	.02		
Jan 31	.18		

What distinguishes the major mid-February episode are uniform meteorological conditions across the entire WHITEX study region. Figure 4.22 shows wind vectors on an hourly basis for the major and gradient sites on JD=43, a day of bad visibility at Page, Hopi, Canyonlands, Bullfrog and elsewhere. The winds are light and variable and exhibit a diurnal "sloshing" back and forth indicating stagnant conditions. The episode is abruptly terminated before dawn on JD=45 by the passage of a strong front as Figure 4.23 shows. This episode varies considerably with other minor episodes that occurred during the WHITEX period. For example, Figure 4.24 shows the wind vectors on JD=28, a day of impaired visibility at Bullfrog and Page, conditions are stagnant at Bullfrog and Page until noon when a fast moving front cleans out the atmosphere. However, on JD=28, many sites are experiencing very windy conditions throughout the day; at Hopi, very high concentrations of fine soil and increased extinction were reported that afternoon.

Appendix 6E has daily wind vectors for all days of the WHITEX study period and Appendix 6F has plots of the upper air soundings. The upper air data were collected from soundings 3 times daily at 0600, 1100, and 1700 hours at Canyonlands and Page.

4.6 Relationships Between Variables

Insight into the relationships between primary emissions and their secondary byproducts can be gained by comparing the fully scaled CD_4 and trace element data with ammonium sulfate, ammonium nitrate, total sulfur, total nitrate nitrogen, and other components of fine mass. It is also of interest to examine relationships between trace elements, secondary aerosols and fully scaled CD_4 concentrations. Only at Page and Hopi Point are there an adequate number of CD_4 samples analyzed to scatter against the other data.

All data presented in this section that are not of 12 hour duration will be either averaged from 6 hour data to 12 hour data or disaggregated from 24 hour data to to 12 hour values. The 6 hour

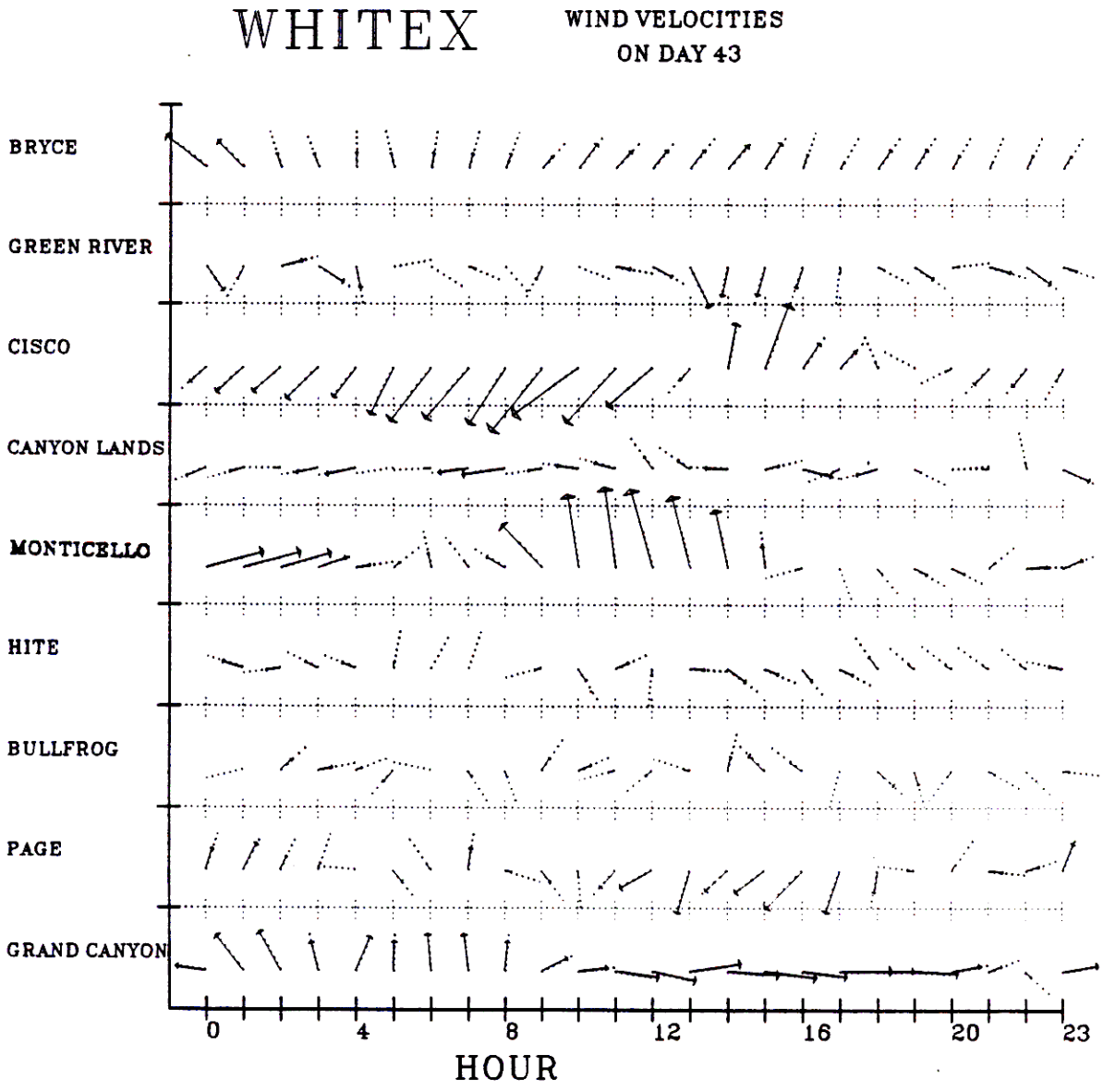

Figure 4.22: Wind velocities across WHITEX study region on Julian Day 43. The length of the dotted line is scaled to 5 mph.

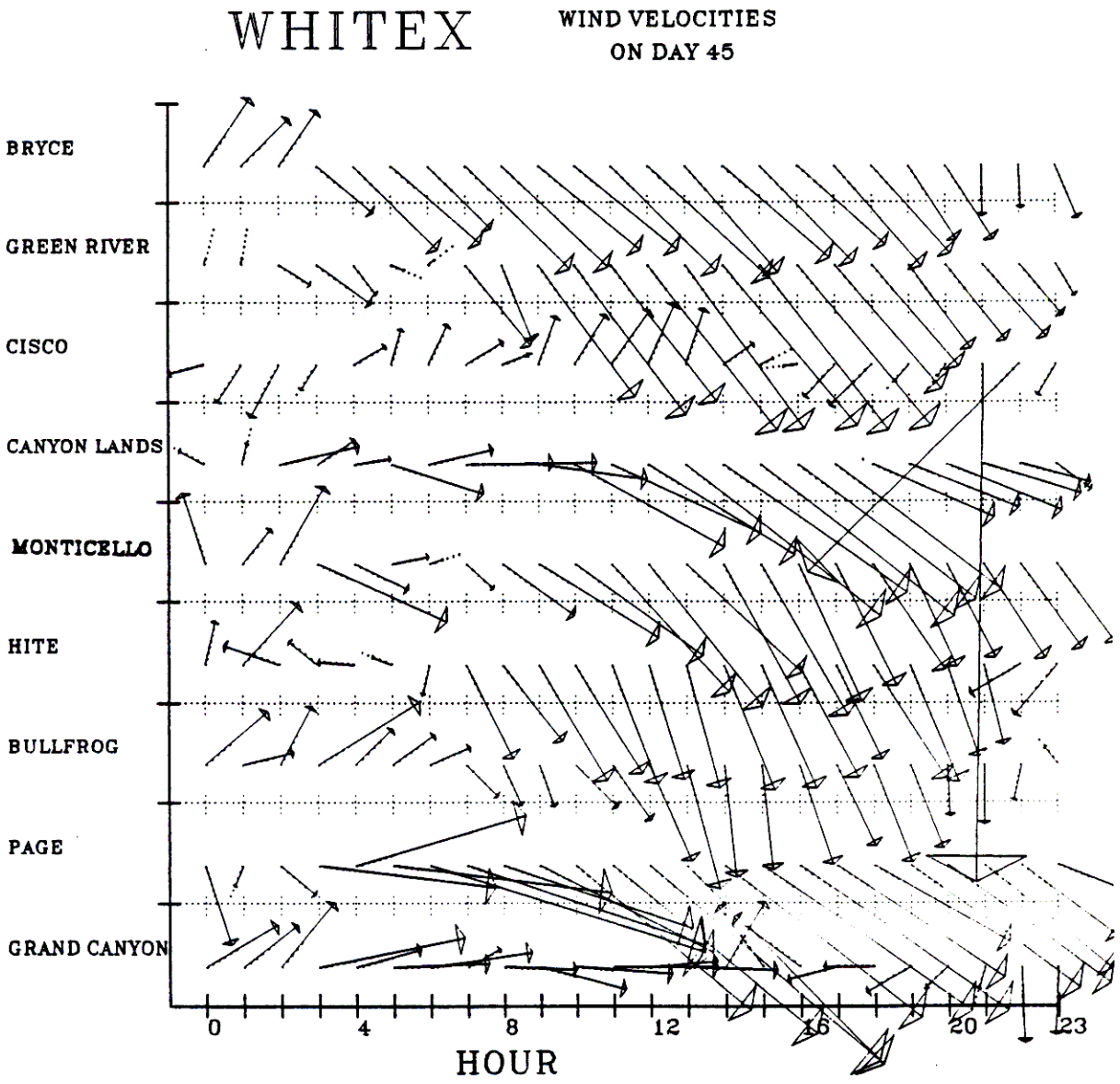

Figure 4.23: Wind velocities across WHITEX study region on Julian Day 45. The length of the dotted line is scaled to 5 mph.

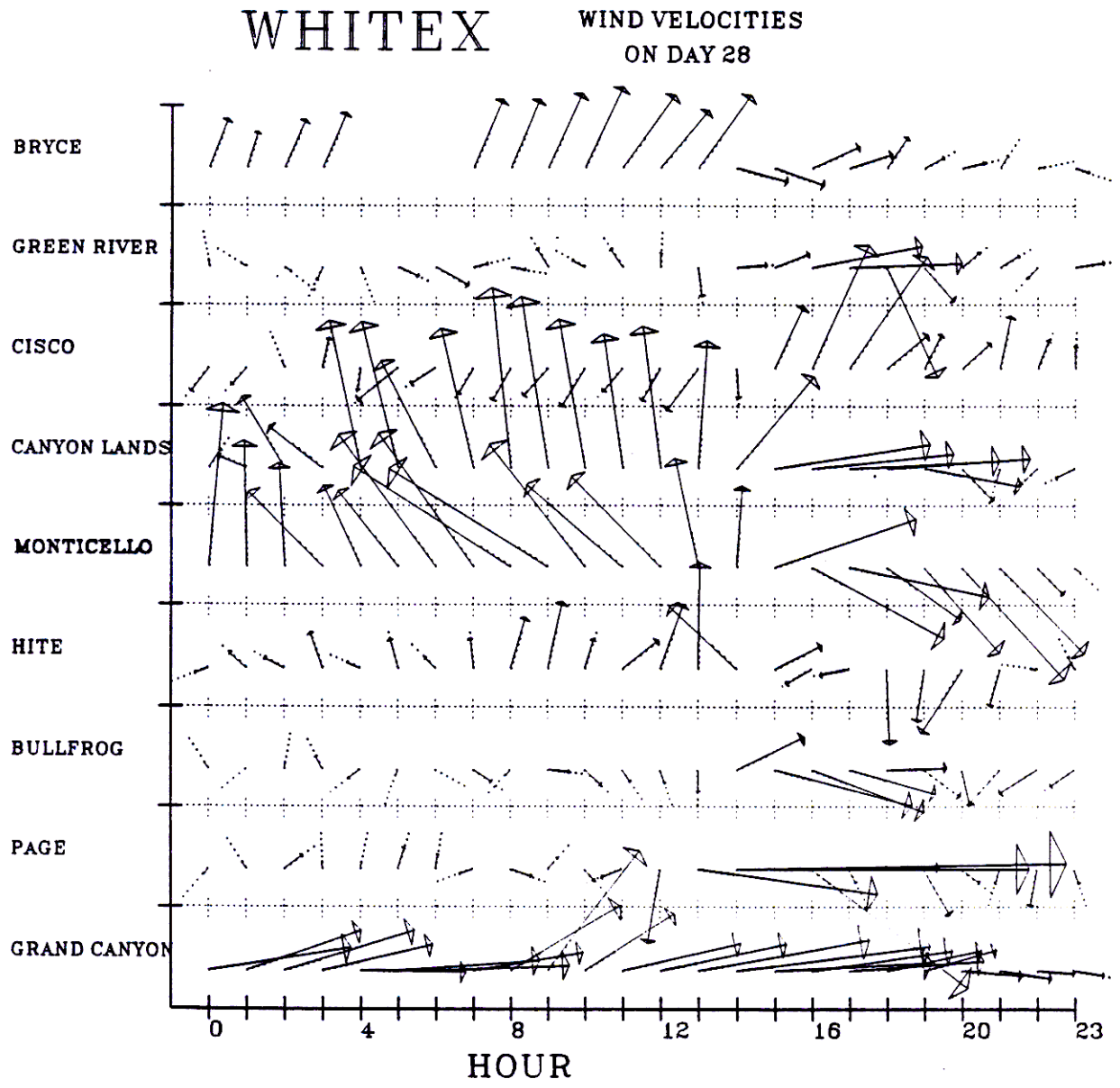

Figure 4.24: Wind velocities across WHITEX study region on Julian Day 28. The length of the dotted line is scaled to 5 mph.

data that are averaged consists of ammonium sulfate, total sulfur, sulfate sulfur, and SO_2 sulfur. The 24 hour data that are disaggregated are ammonium nitrate, total nitrate and the SCISAS selenium at Hopi Point.

Beginning with Page, the relationships of fully scaled CD_4 on the x-axis to sulfate sulfur, total sulfur, nitrate nitrogen, and total nitrate nitrogen on the y-axis is shown in Figure 4.25. The relationship of sulfate sulfur to CD_4 appears to be strong except for the existence of 4 "outliers" in which the ratio of sulfate sulfur to CD_4 is much higher than for the rest of the points. In the scatter plot of total sulfur to CD_4, there are no such outliers. Particulate nitrate nitrogen and total nitrate nitrogen appear to have very weak or no relationship to CD_4.

Figures 4.26 and 4.27 have the elements selenium and arsenic substituted for fully scaled CD_4, respectively. Selenium (Figure 4.26) shows similar relationships to total sulfur and sulfate sulfur as does fully scaled CD_4, with the strongest relationship being between total sulfur and selenium. The plots of selenium *vs* particulate nitrate nitrogen or selenium *vs* total nitrate nitrogen exhibit much more scatter.

Arsenic (Figure 4.27) shows some apparent relationship to both sulfate sulfur and total sulfur, however there are some outliers which exist in both plots. Stronger relationships between arsenic and particulate nitrate nitrogen, and arsenic to total nitrate nitrogen are suggested even though there is much scatter present.

Figure 4.28 has scatter plots of fully scaled CD_4 on the x-axis against the remaining components of fine mass which are: light absorbing carbon, organic carbon, and, fine soil. There are only weak if any relationships between CD_4 and these components of fine mass. Similarly, the trace elements selenium and arsenic as shown in Figures 4.29 and 4.30 do not appear to be strongly related to any of the remaining components of fine mass.

Figure 4.31 has scatter plots of fully scaled CD_4 on the x-axis against selenium, arsenic, copper, zinc, and lead on the y-axis. Only selenium exhibits a strong relationship with CD_4. For a more complete discussion of the relationship between selenium and CD_4, the reader is referred to Section 7.2.3 where a discussion on the scaling of the CD_4 data is given.

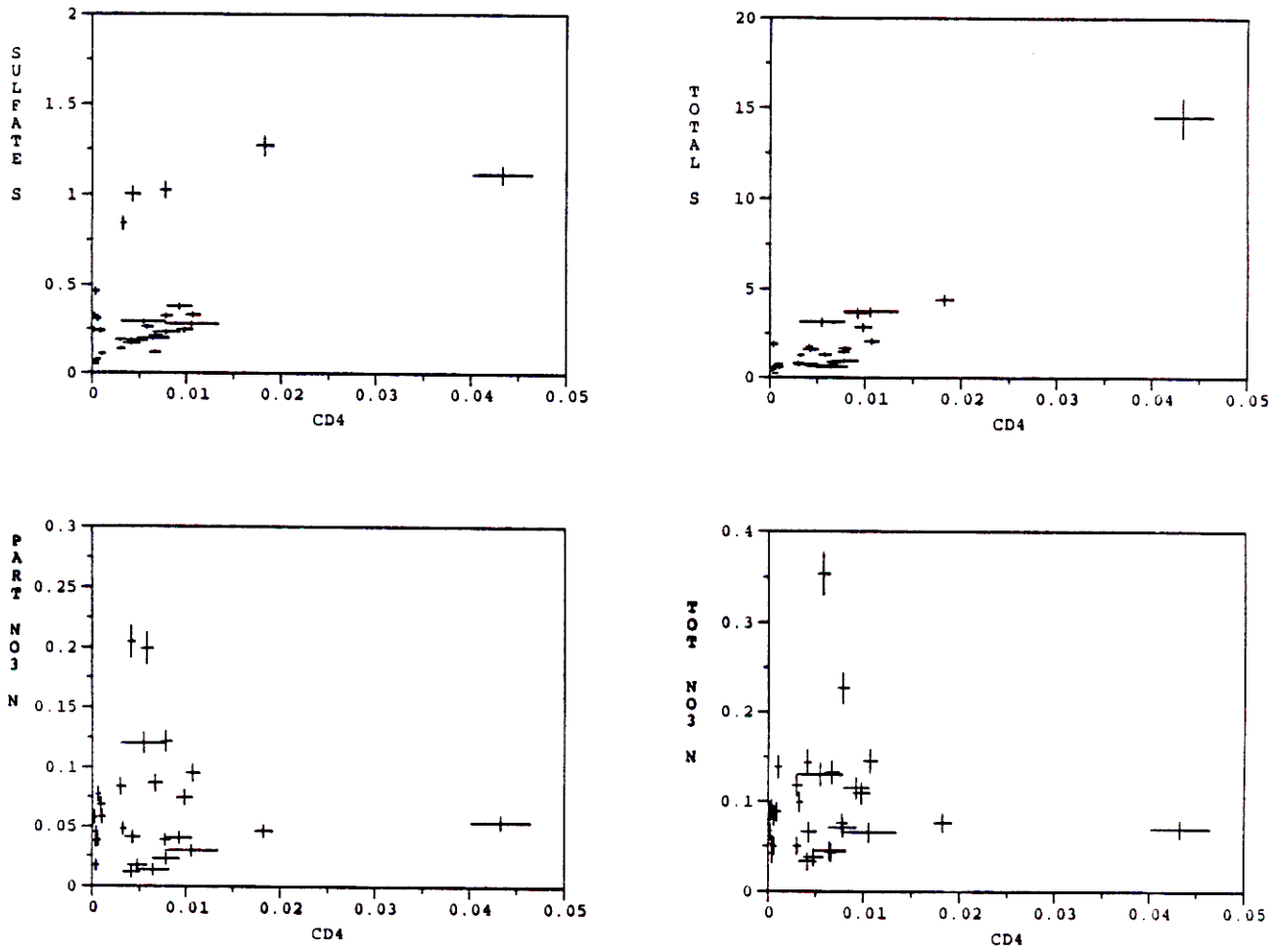

Figure 4.25: Scatter plots of fully scaled CD_4 (ppt) against sulfate sulfur, total sulfur, particulate nitrate nitrogen, and total nitrate nitrogen ($\mu g/m^3$) at Page.

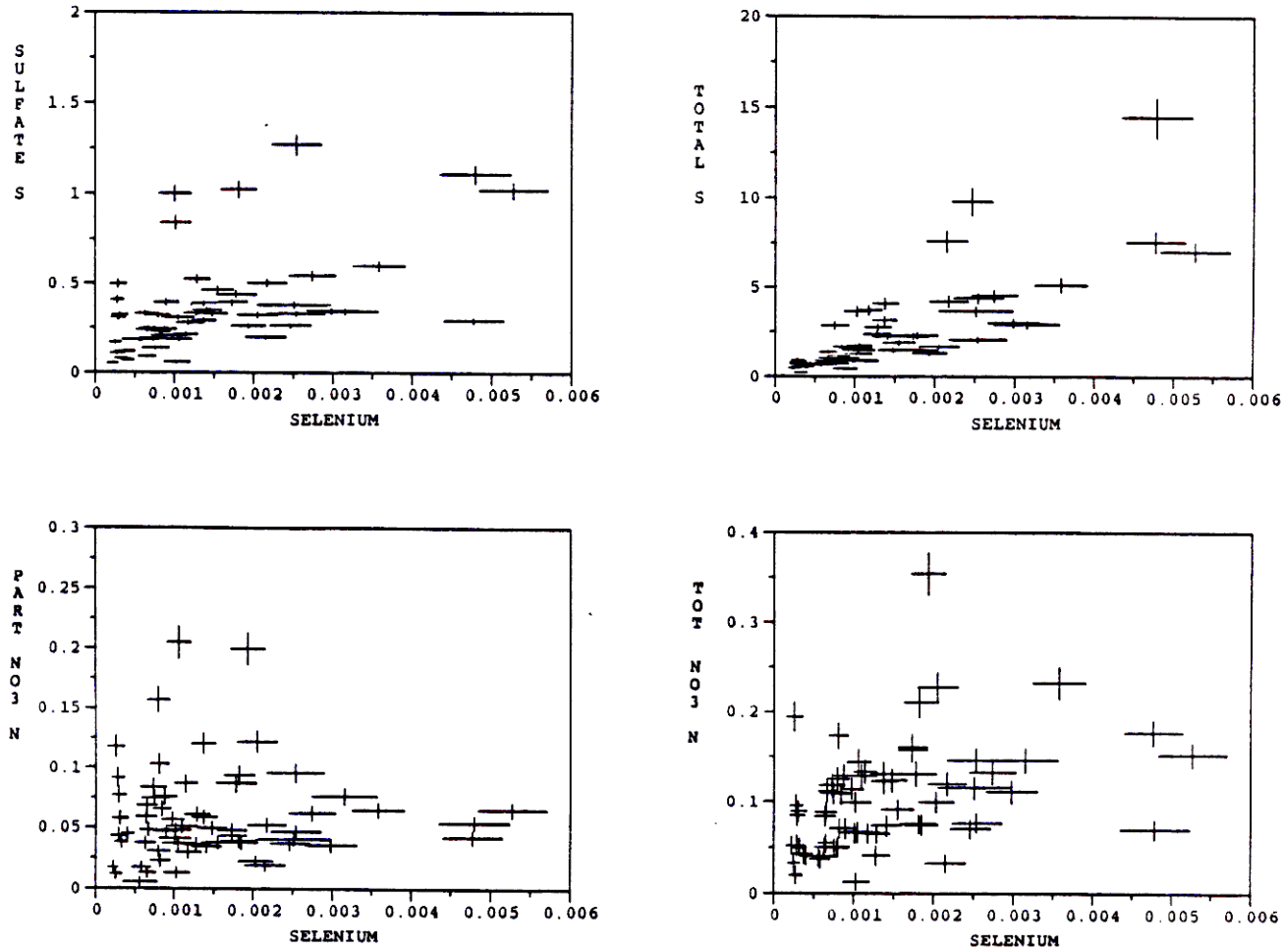

Figure 4.26: Scatter plots of selenium ($\mu g/m^3$) against sulfate sulfur, total sulfur, particulate nitrate nitrogen, and total nitrate nitrogen ($\mu g/m^3$) at Page.

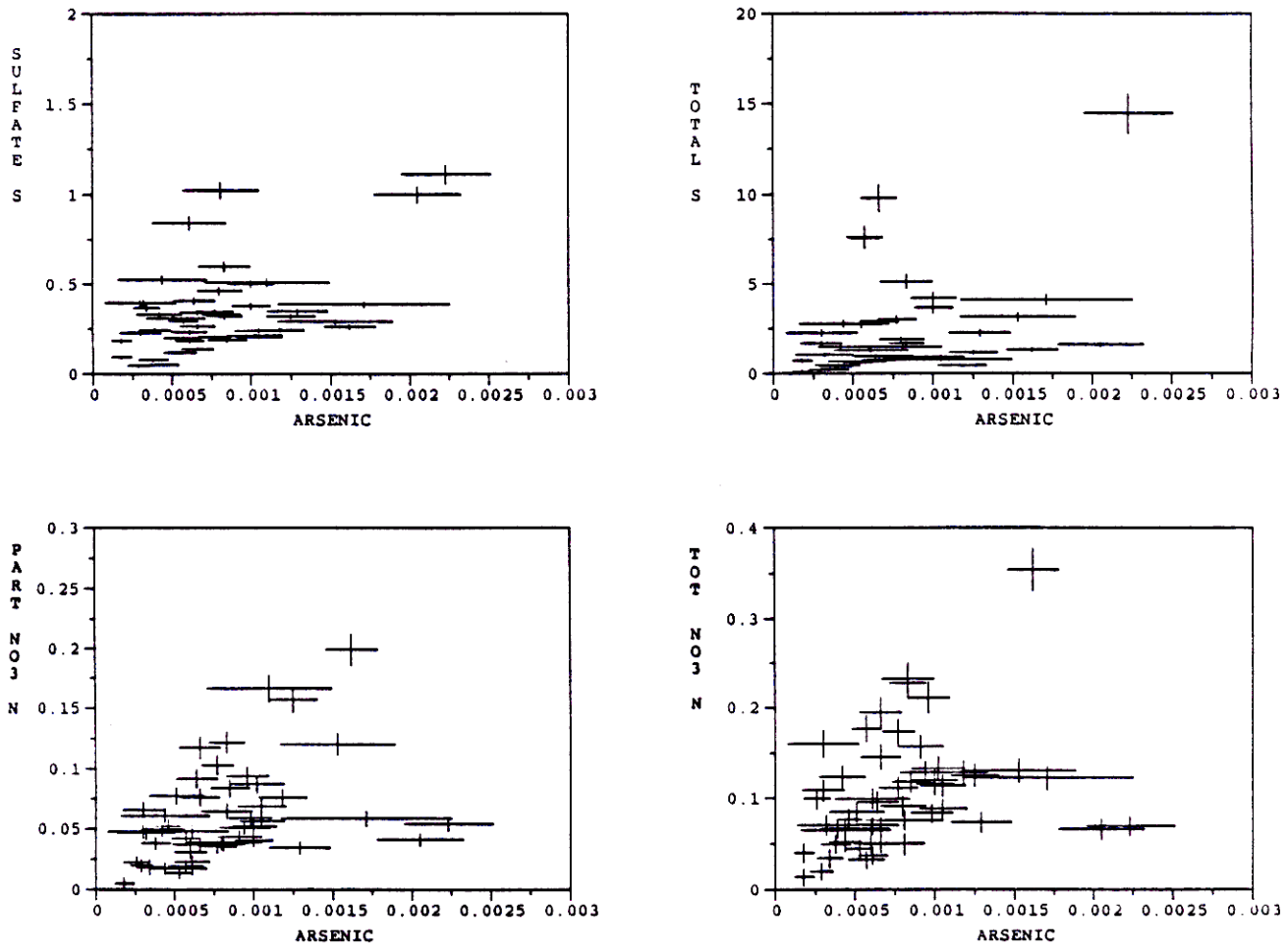

Figure 4.27: Scatter plots of arsenic ($\mu g/m^3$) against sulfate sulfur, total sulfur, particulate nitrate nitrogen and total nitrate nitrogen ($\mu g/m^3$) at Page.

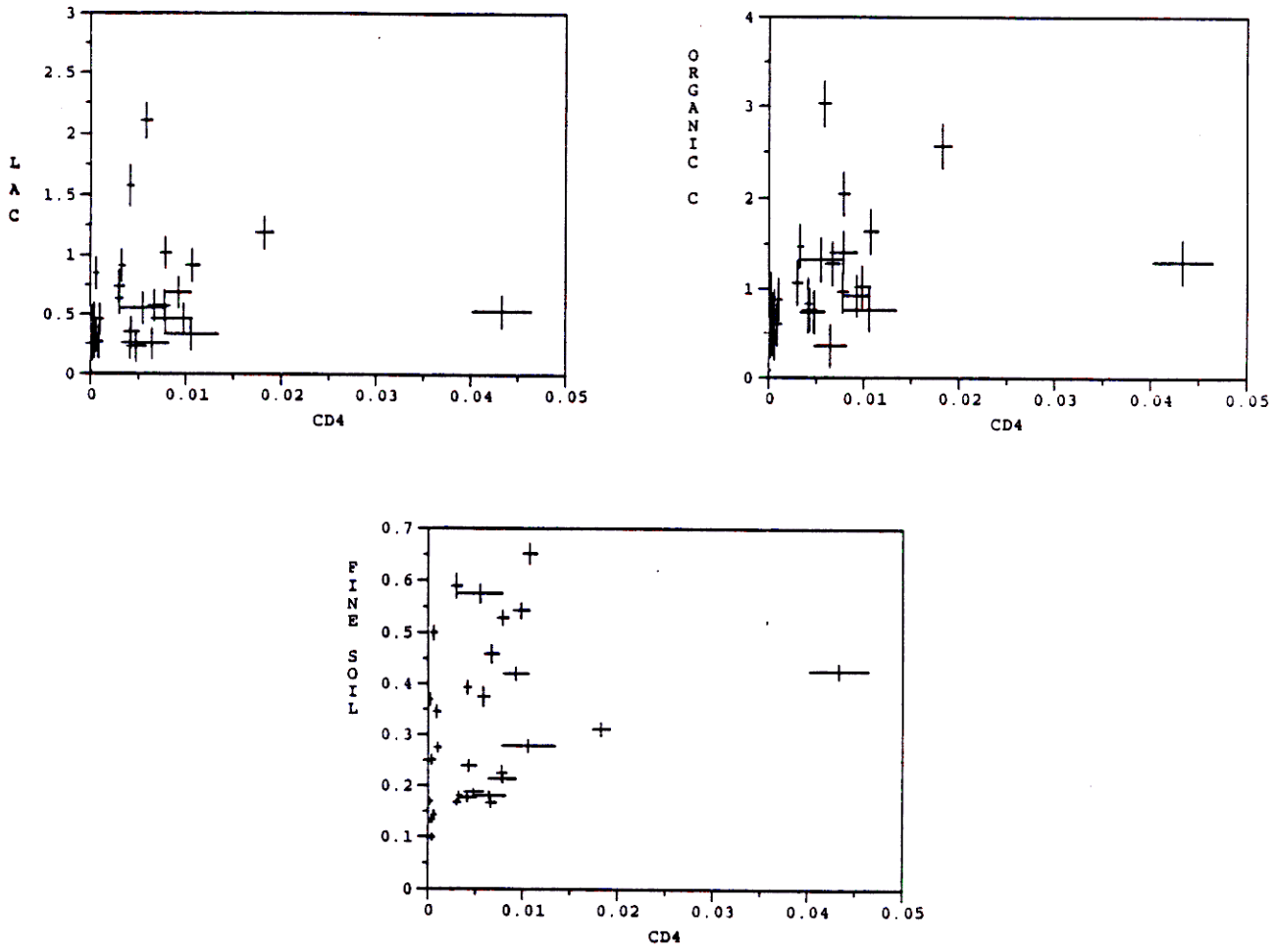

Figure 4.28: Scatter plots of fully scaled CD_4 (ppt) against light absorbing carbon, organic carbon and fine soil ($\mu g/m^3$) at Page.

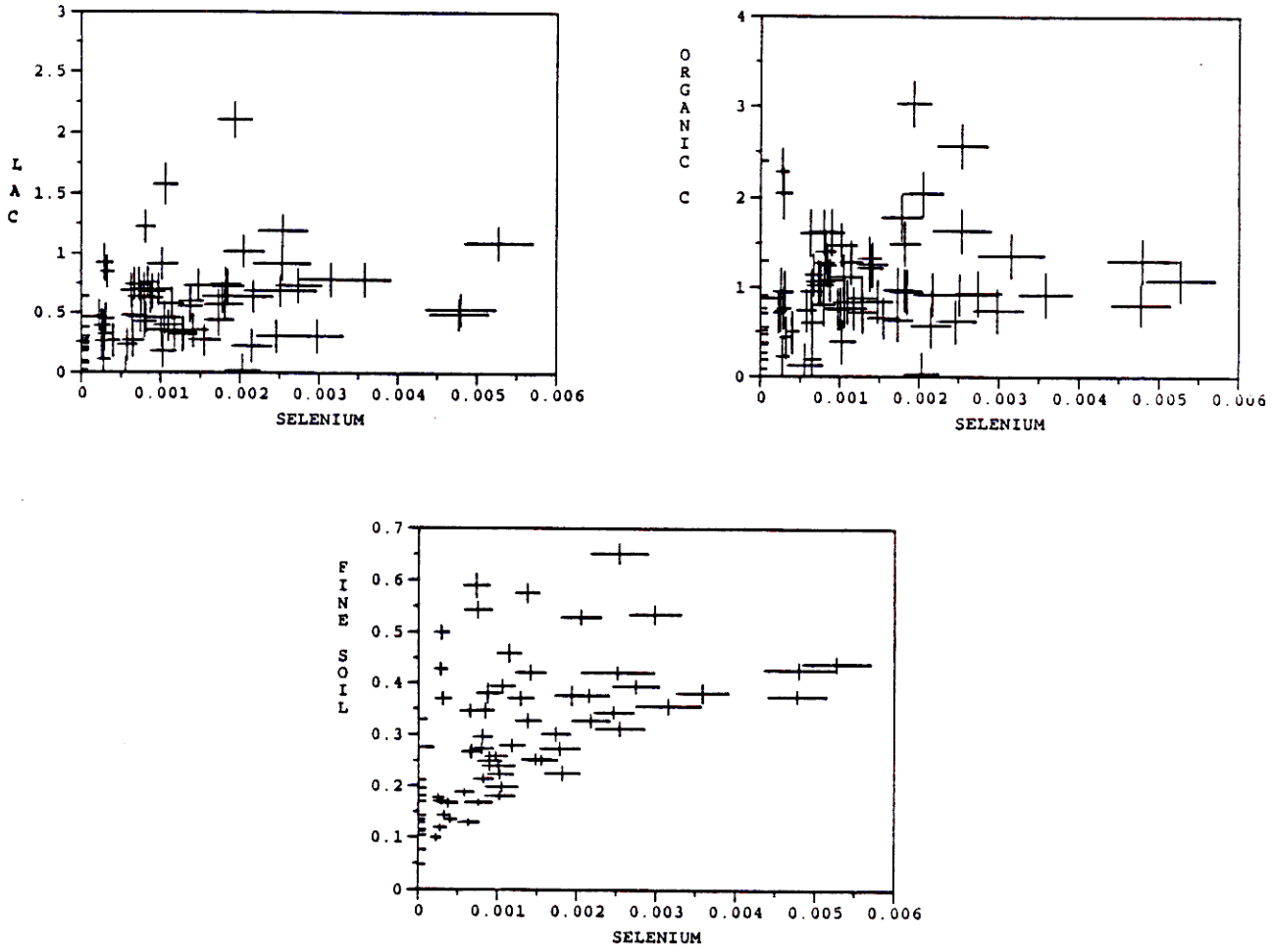

Figure 4.29: Scatter plots of selenium ($\mu g/m^3$) against light absorbing carbon, organic carbon and fine soil ($\mu g/m^3$) at Page.

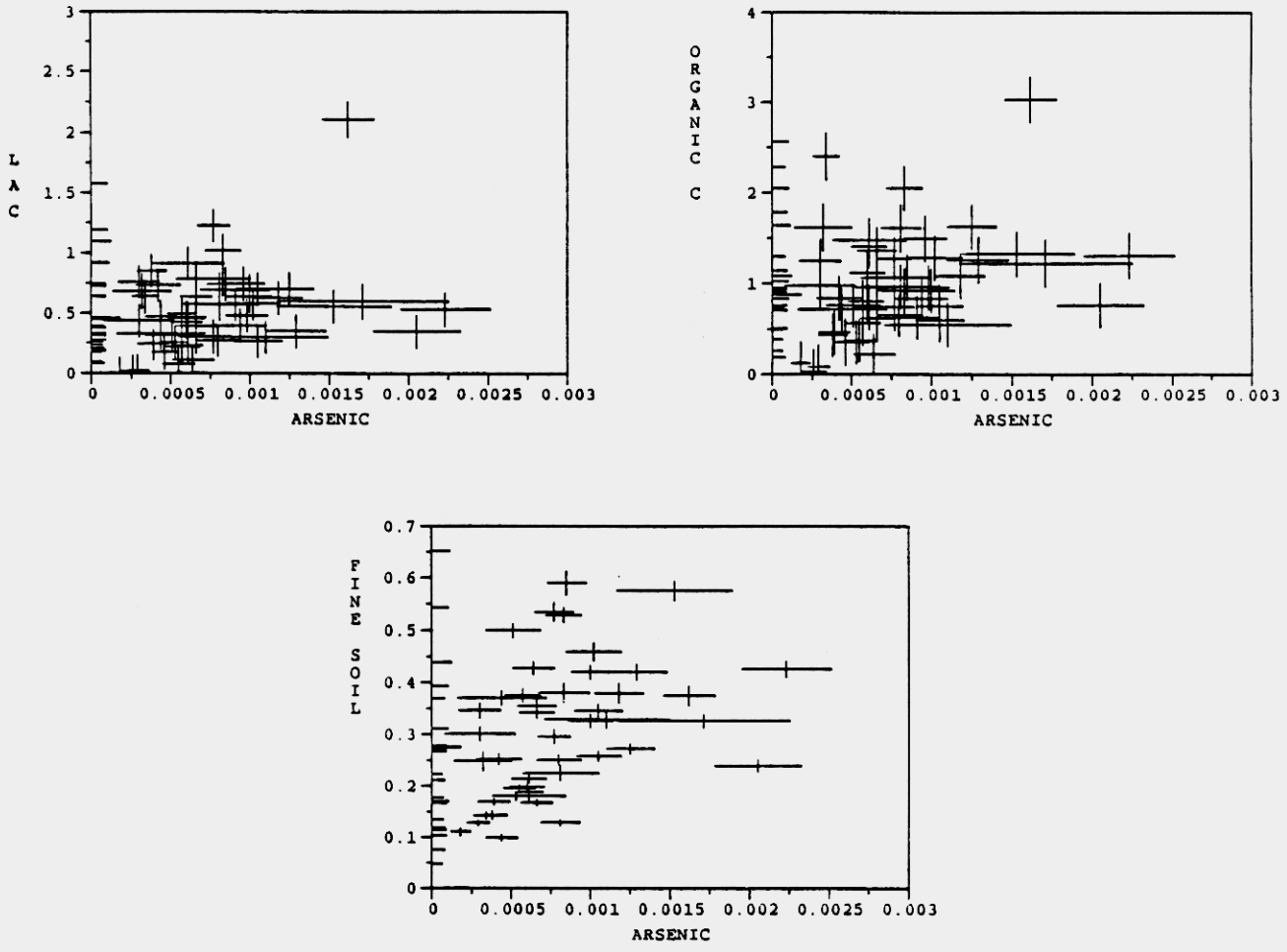

Figure 4.30: Scatter plots of arsenic ($\mu g/m^3$) against light absorbing carbon, organic carbon and fine soil ($\mu g/m^3$) at Page.

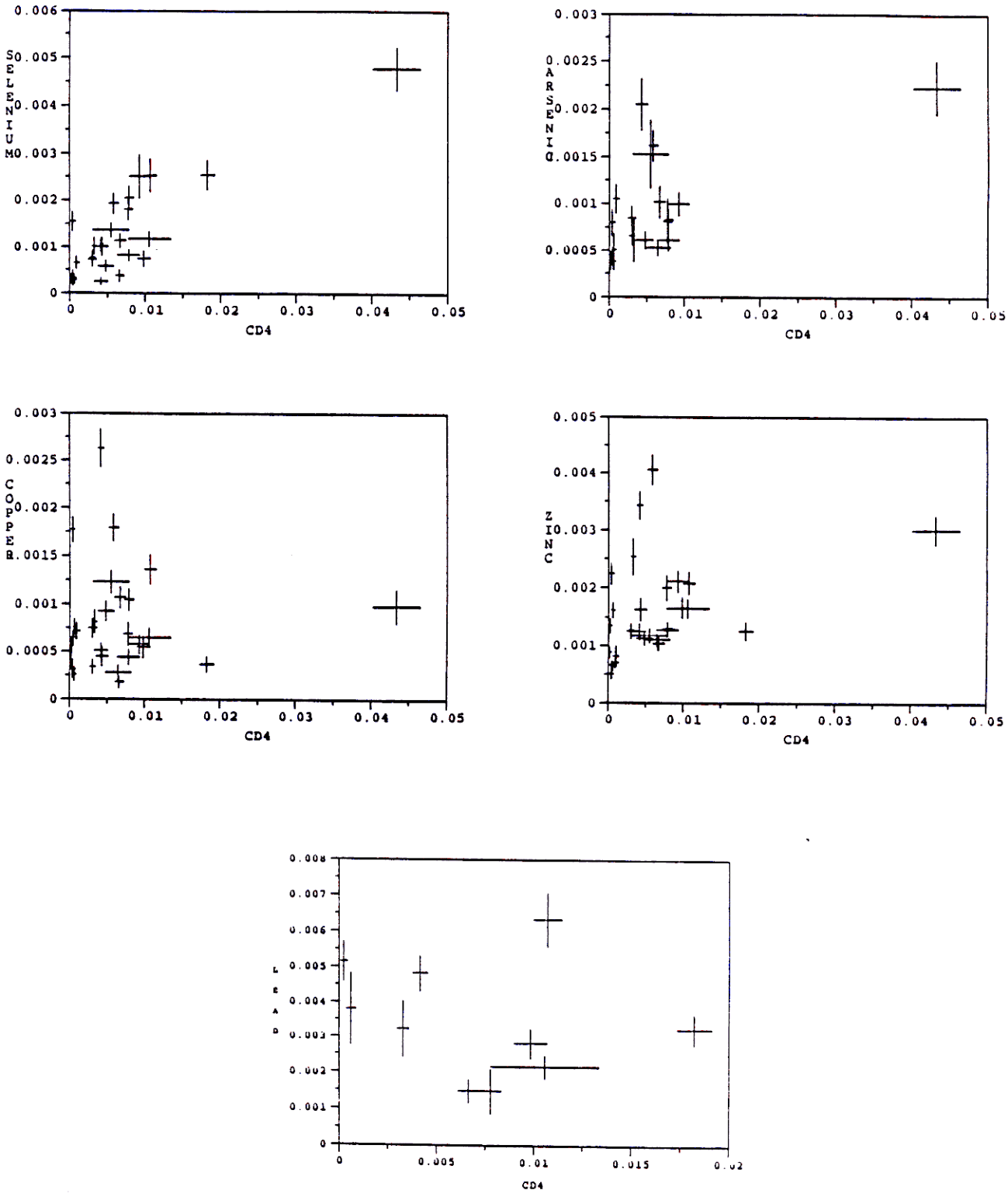

Figure 4.31: Scatter plots of fully scaled CD_4 (ppt) against selenium, arsenic, copper, zinc, and lead ($\mu g/m^3$) at Page.

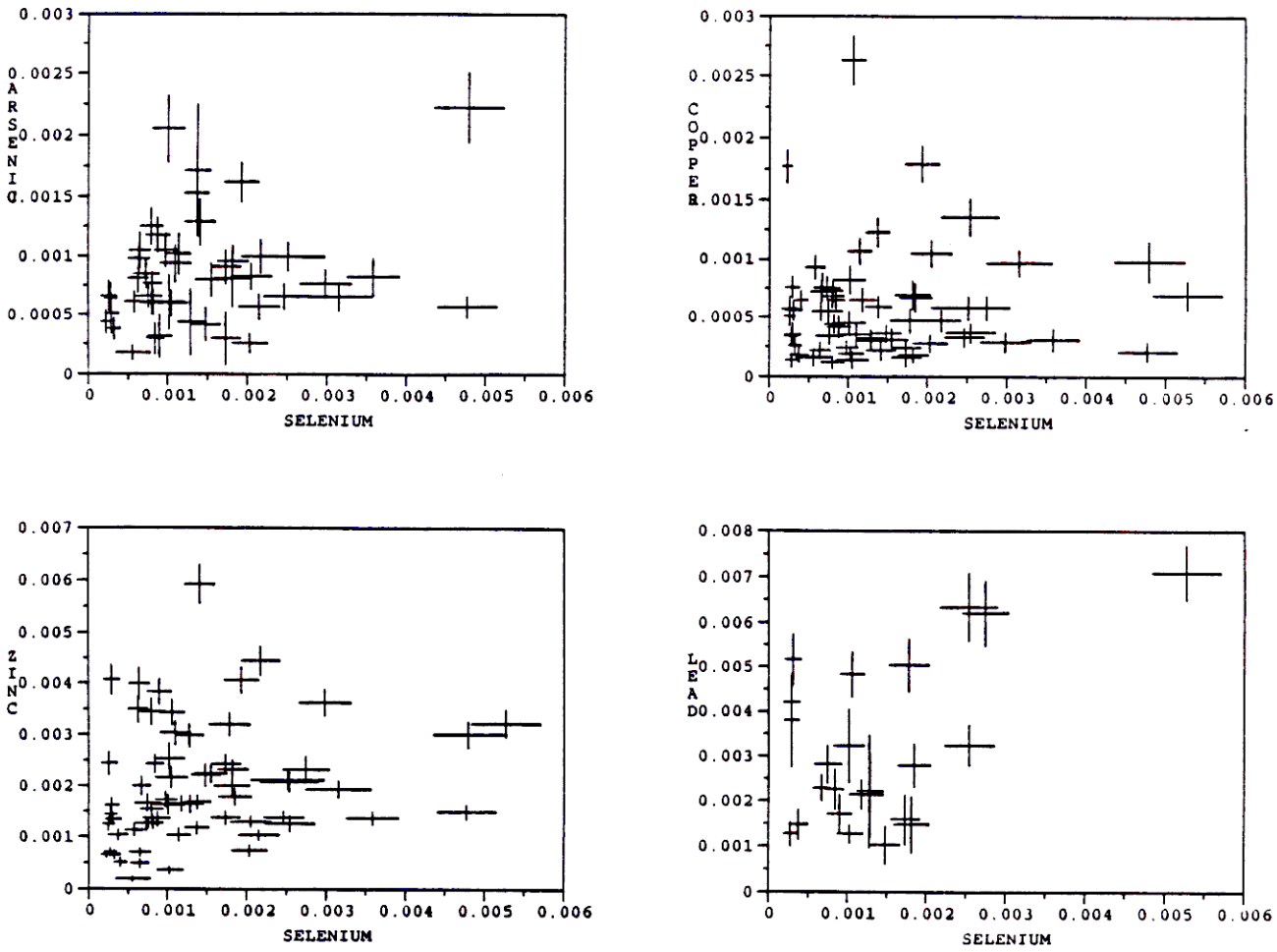

Figure 4.32: Scatter plots of selenium ($\mu g/m^3$) against arsenic, copper, zinc, and lead ($\mu g/m^3$) at Page.

Figure 4.32 shows the scatter plots of selenium on the x-axis against arsenic, copper, zinc, and lead on the y-axis. The relationship between selenium and all of the other trace elements appears to be quite weak. This suggests that the trace elements other than selenium also originate from sources other than NGS. Figures 4.33 and 4.34 show scatter plots of the trace elements other than selenium. Figure 4.33 has arsenic on the x-axis and copper, zinc, and lead on the y-axis. It is difficult to discern much relationship here, although there appears to be some correlation between zinc and arsenic. Figure 4.34 has scatter plots of zinc against copper, lead against copper, and lead against zinc. Except for one outlier point it appears that there is a correlation between lead and copper while there is none if any between zinc and copper or between lead and zinc.

At Hopi Point, some of the same relationships of fully scaled CD_4, selenium, and arsenic to sulfates, nitrates, total sulfur, and total nitrate nitrogen exist as are evident at Page. Figure 4.35 has the scatter plots of fully scaled CD_4 on the x-axis against sulfate sulfur, total sulfur, particulate nitrate nitrogen, and total nitrate nitrogen on the y-axis. As at Page (Figure 4.25), sulfate sulfur at Hopi Point shows a noticeable relationship with CD_4. The relationship of CD_4 to total sulfur is evident at Hopi Point. The one outlier on the total sulfur *vs* CD_4 plot is due to a high SO_2 concentration on JD 35 (Figure 4.4).

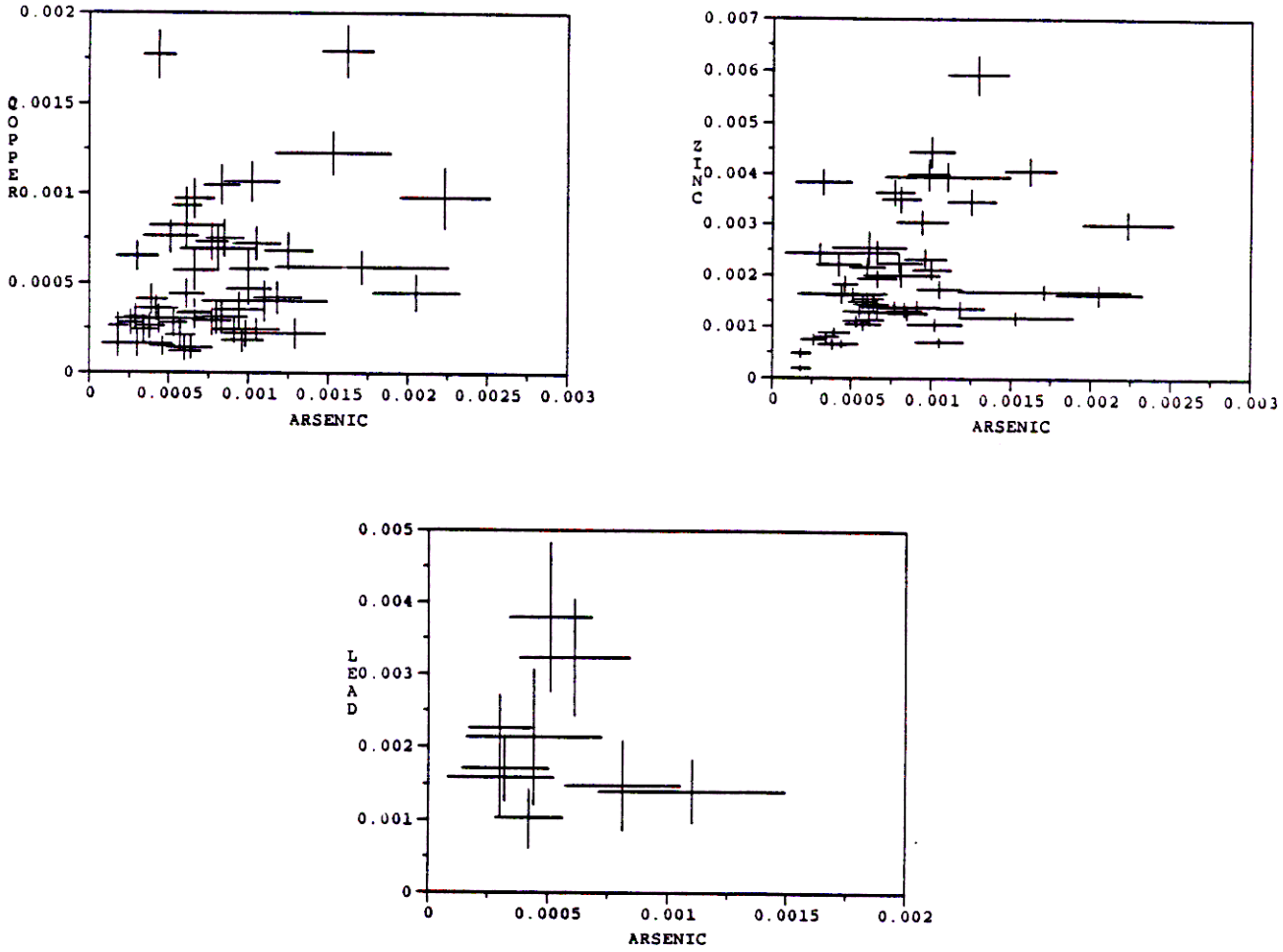

Figure 4.33: Scatter plots of arsenic ($\mu g/m^3$) against copper, zinc, and lead ($\mu g/m^3$) at Page.

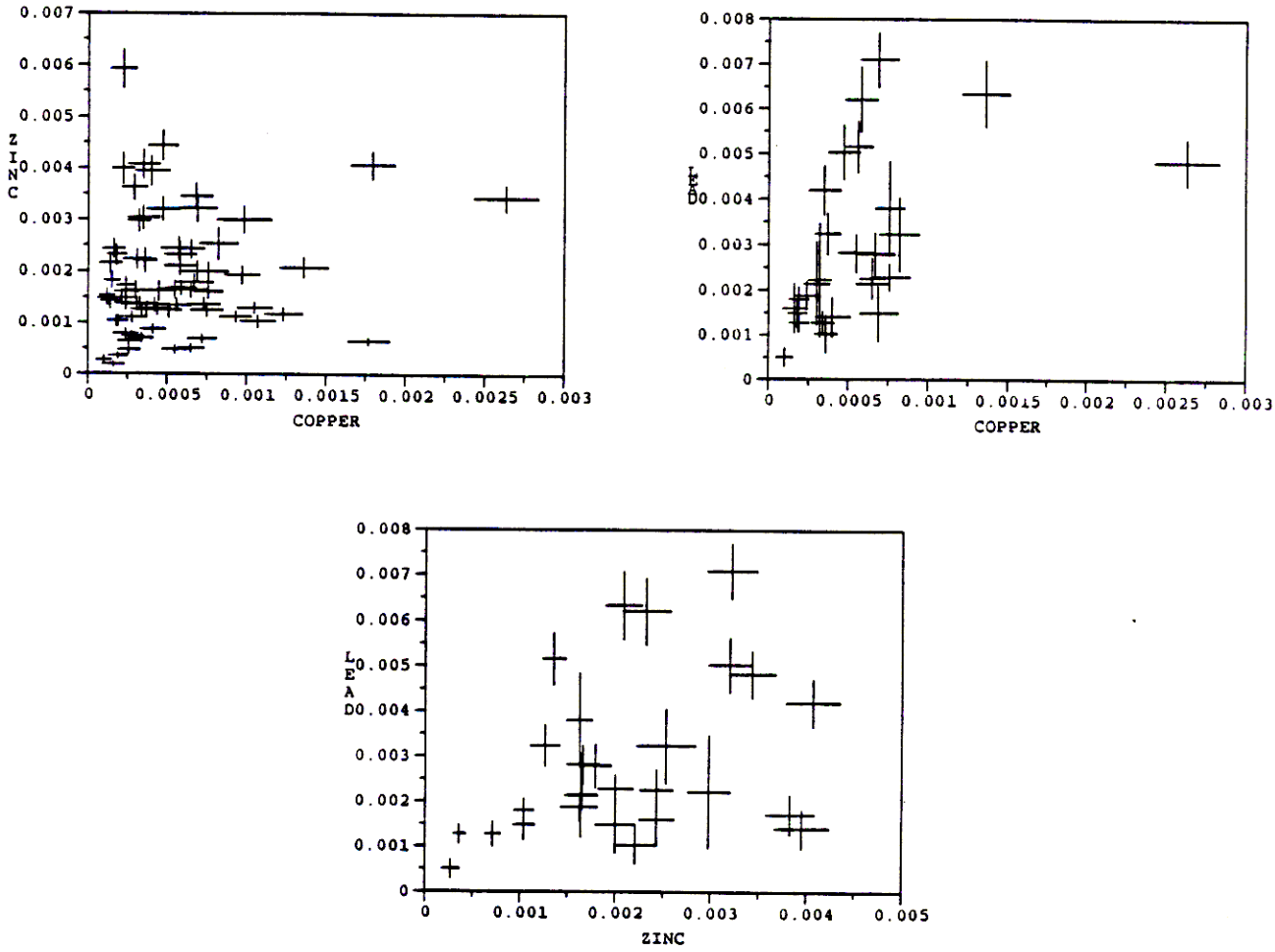

Figure 4.34: Scatter plots of copper ($\mu g/m^3$) against zinc and lead ($\mu g/m^3$) and scatter plot of zinc against lead at Page.

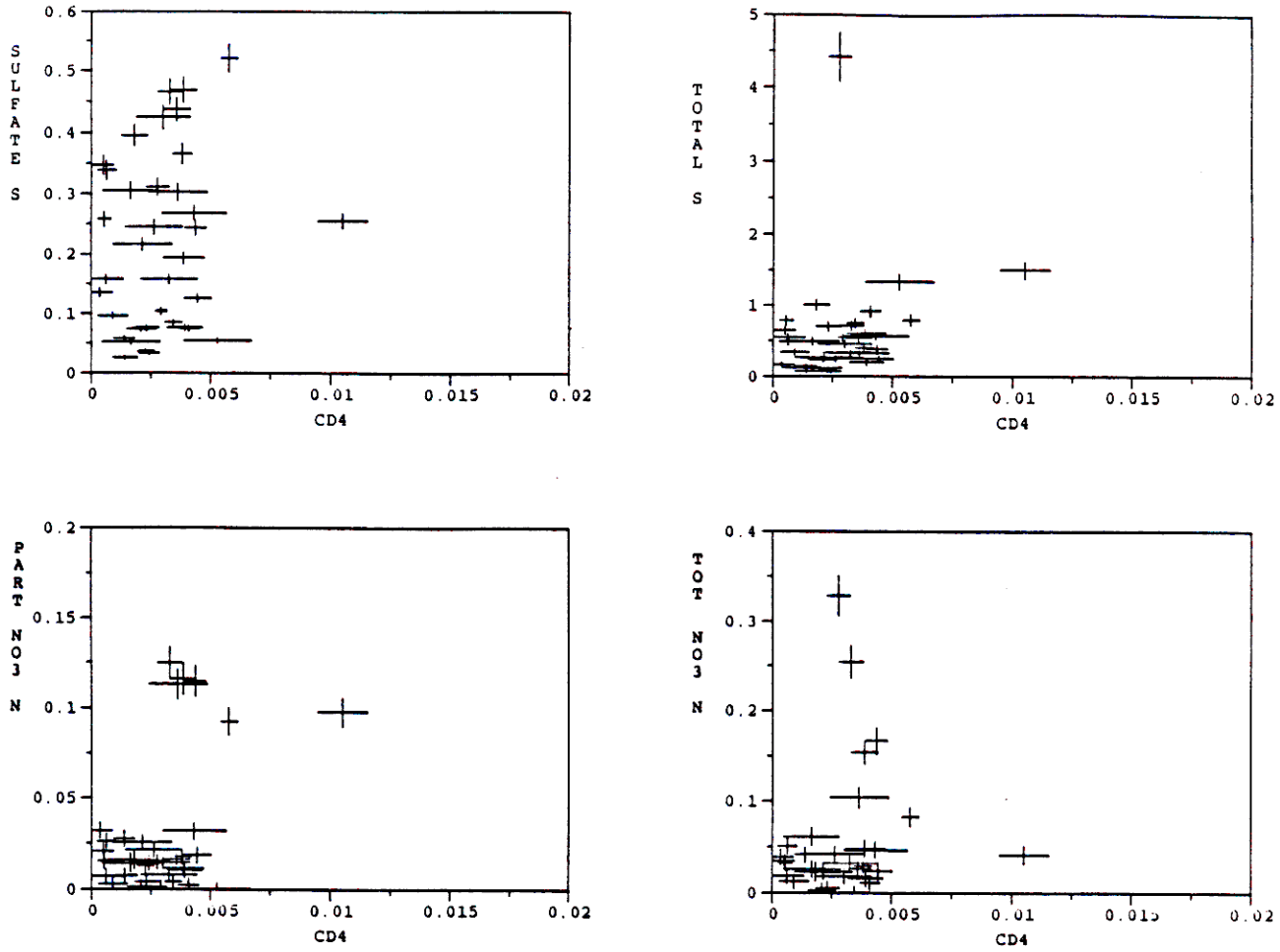

Figure 4.35: Scatter plots of fully scaled CD_4 (ppt) against sulfate sulfur, total sulfur, particulate nitrate nitrogen, and total nitrate nitrogen ($\mu g/m^3$) at Hopi Point.

Figure 4.36 has the scatter plots of selenium on the x-axis against sulfate sulfur, total sulfur, particulate nitrate nitrogen, and total nitrate nitrogen on the y-axis. The plot of sulfate sulfur *vs* selenium shows much scatter, however, some correlation seems evident. Except for the SO_2 induced outlier point on JD 35 the relationship between selenium and total sulfur appears to be quite strong. The plot of selenium *vs* particulate nitrate nitrogen suggests that there may be two different populations as there is a cluster of 5 elevated nitrogen and selenium points. The relationship between total nitrate nitrogen and selenium suggests the same although the cluster is not as well defined.

Figure 4.37 has the scatter plots of arsenic on the x-axis against sulfate sulfur, total sulfur, nitrate nitrogen, and total nitrogen on the y-axis. The relationship of sulfate sulfur to arsenic is interesting in that the lower right triangular portion of the plot is empty. This suggests that for a any given arsenic concentration, there is a minimum sulfur concentration associated with it. Except for one outlier point, a relationship between total sulfur and arsenic appears to exist without much scatter. The relationships of arsenic to particulate nitrate nitrogen and arsenic to total nitrate nitrogen are apparently weak.

Figure 4.38 shows the scatter plots of fully scaled CD_4 against the other components of fine mass, including light absorbing carbon, organic carbon, and, fine soil. There are no discernable

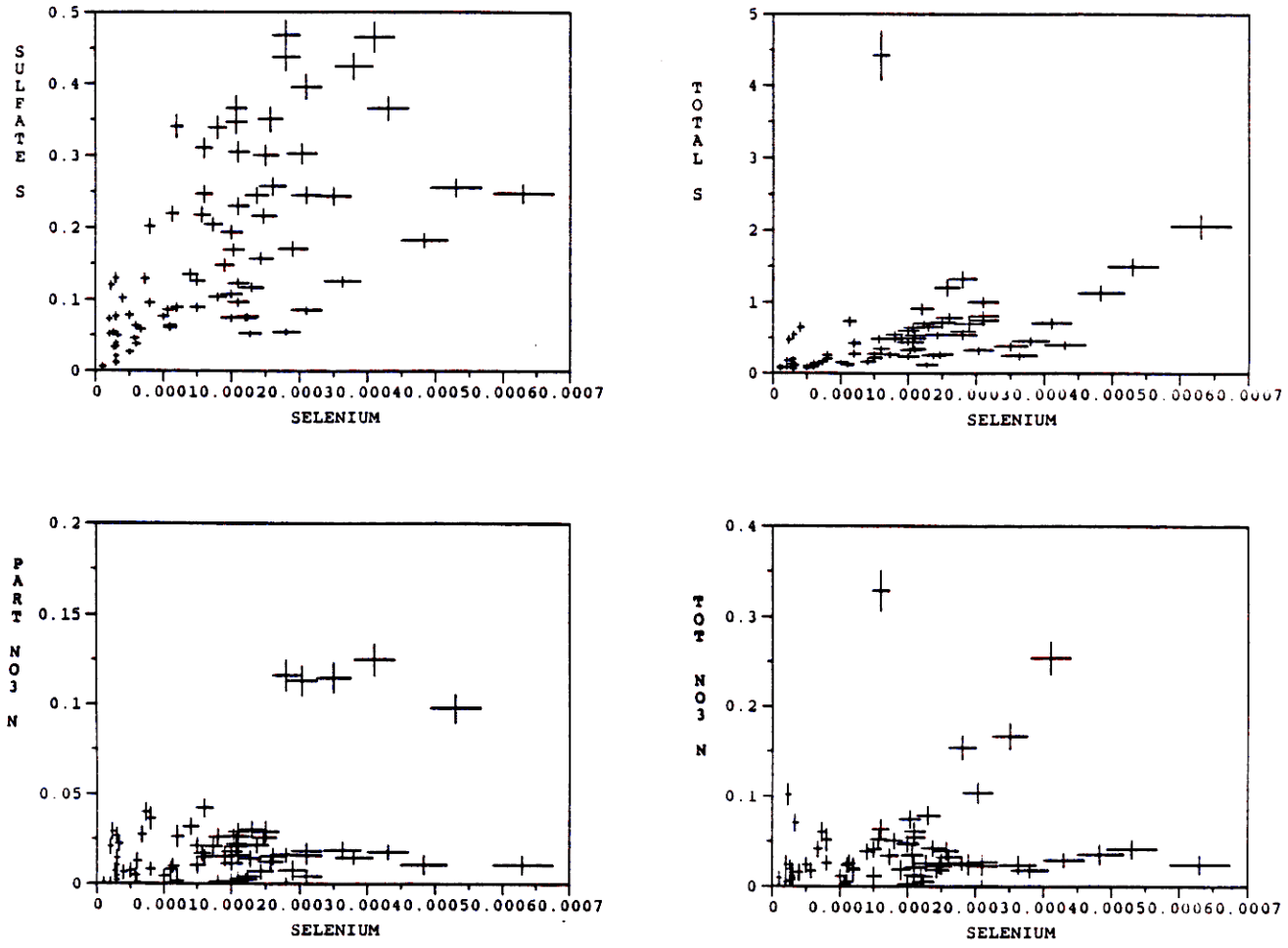

Figure 4.36: Scatter plots of selenium ($\mu g/m^3$) against sulfate sulfur, total sulfur, particulate nitrate nitrogen, and total nitrate nitrogen ($\mu g/m^3$) at Hopi Point.

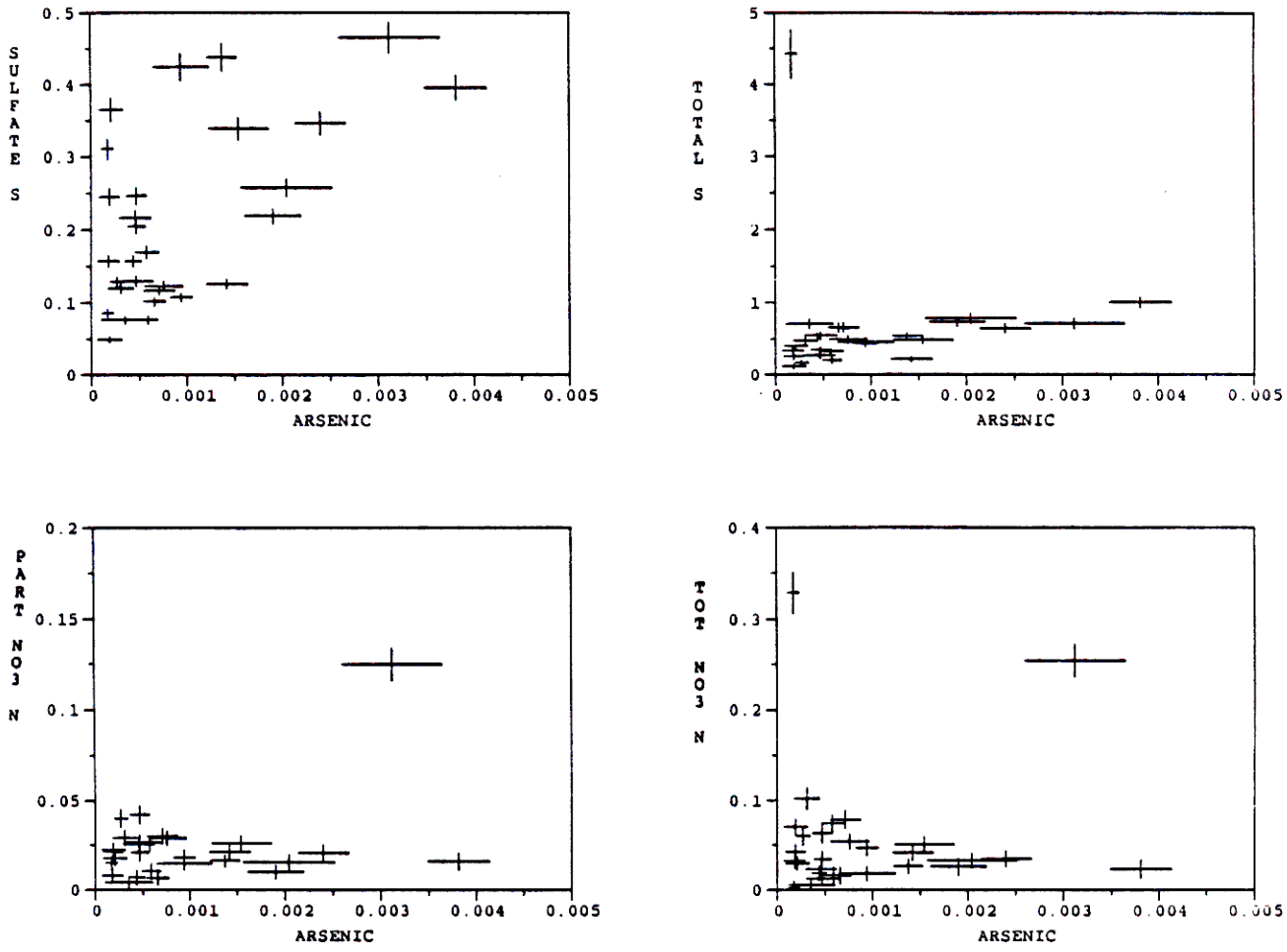

Figure 4.37: Scatter plots of arsenic ($\mu g/m^3$) against sulfate sulfur, total sulfur, particulate nitrate nitrogen and total nitrate nitrogen ($\mu g/m^3$) at Hopi Point.

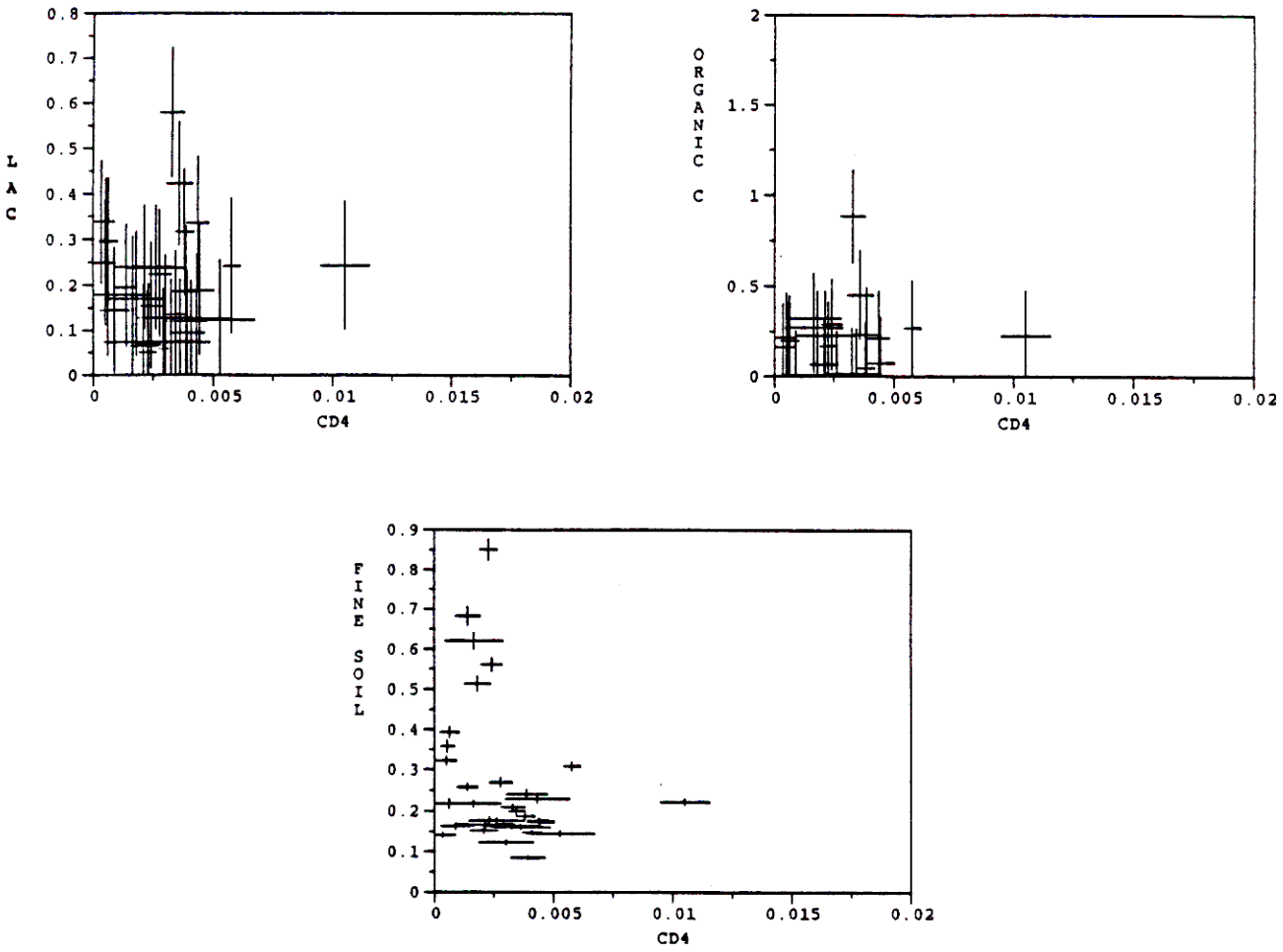

Figure 4.38: Scatter plots of fully scaled CD_4 (ppt) against light absorbing carbon, organic carbon, and fine soil ($\mu g/m^3$) at Hopi Point.

relationships between any of these components and CD_4. Similarly, the same may be said about selenium and arsenic as shown in Figures 4.39 and 4.40, respectively.

The relationship of fully scaled CD_4 to the trace elements selenium, arsenic, copper, zinc, and lead are shown if Figure 4.41. The strongest relationship between is between CD_4 and selenium. The other trace elements (arsenic, copper, zinc, and lead) show weak if any relationships to CD_4. Similarly, selenium does not appear to be related to copper, zinc, or lead (Figure 4.42).

Figure 4.43 has the scatter plots of arsenic on the x-axis against copper, zinc, and lead on the y-axis. All three of these combinations indicate positive correlations with each other. The strongest relationship is between lead and arsenic.

Figure 4.44 shows the relationship of copper to zinc and lead and the relationship of zinc to lead. Once again, all three combinations indicate a positive correlations with each other with the strongest being between lead and copper.

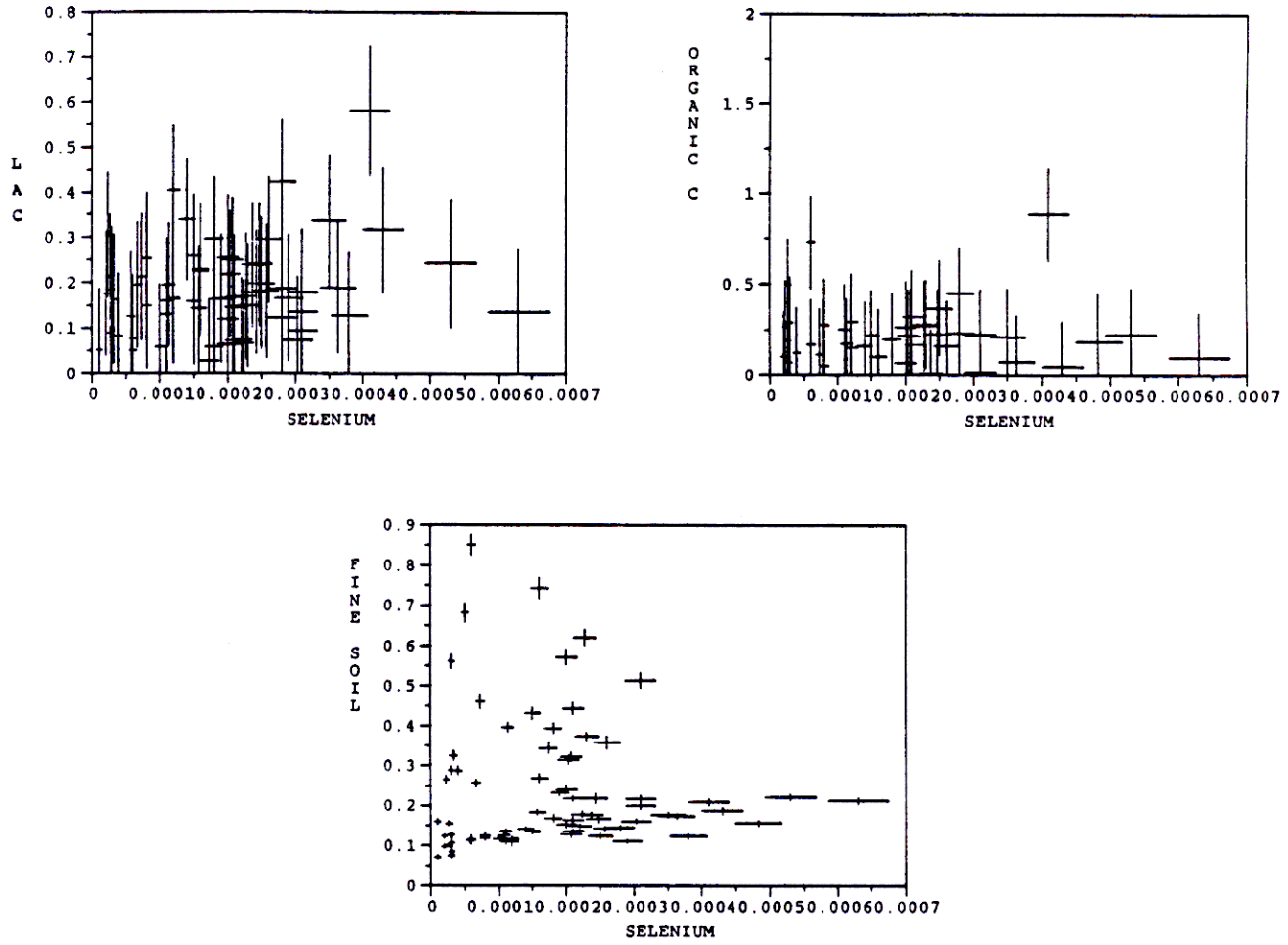

Figure 4.39: Scatter plots of selenium ($\mu g/m^3$) against light absorbing carbon, organic carbon, and fine soil ($\mu g/m^3$) at Hopi Point.

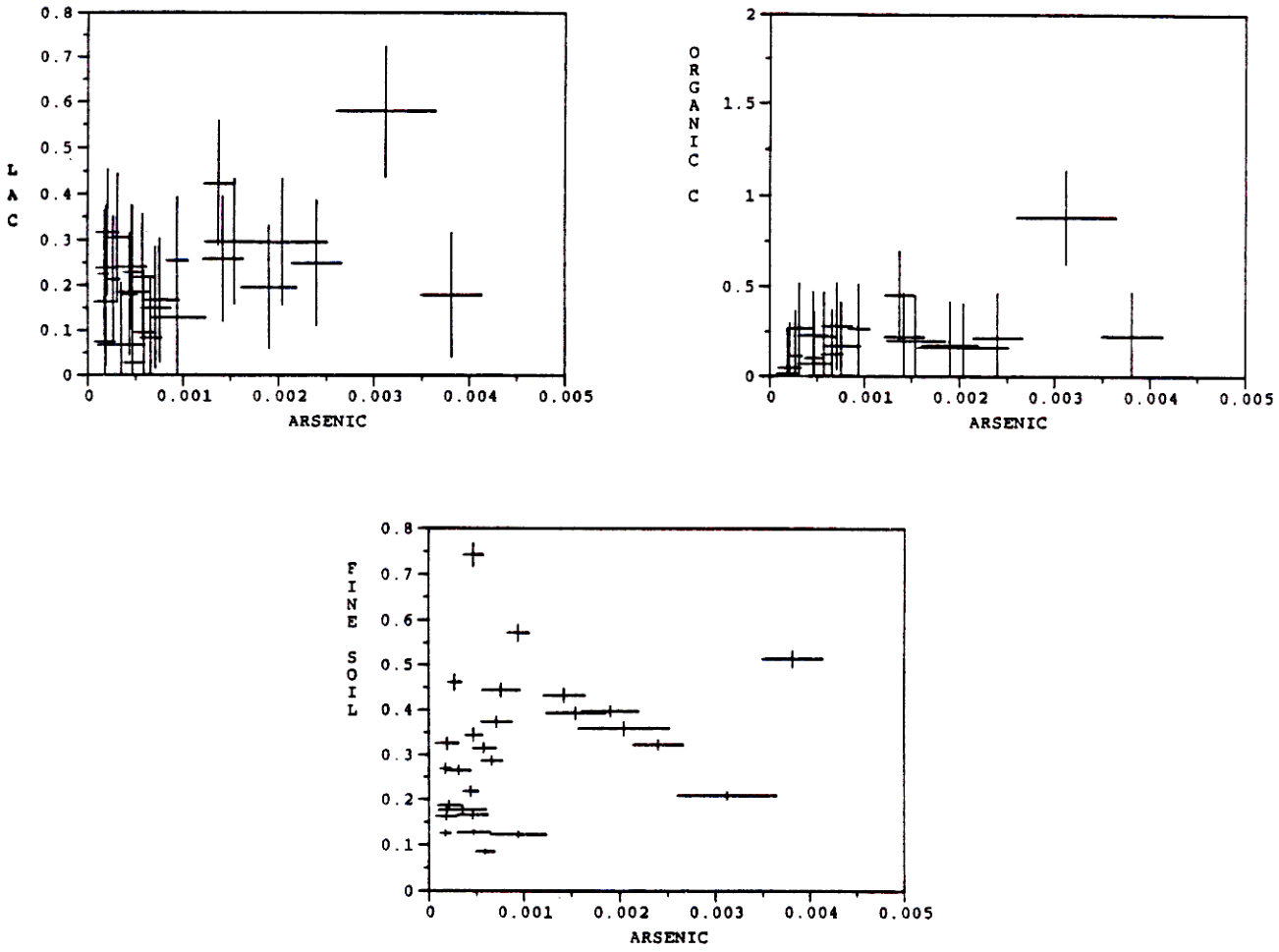

Figure 4.40: Scatter plots of arsenic ($\mu g/m^3$) against light absorbing carbon, organic carbon, and fine soil ($\mu g/m^3$) at Hopi Point.

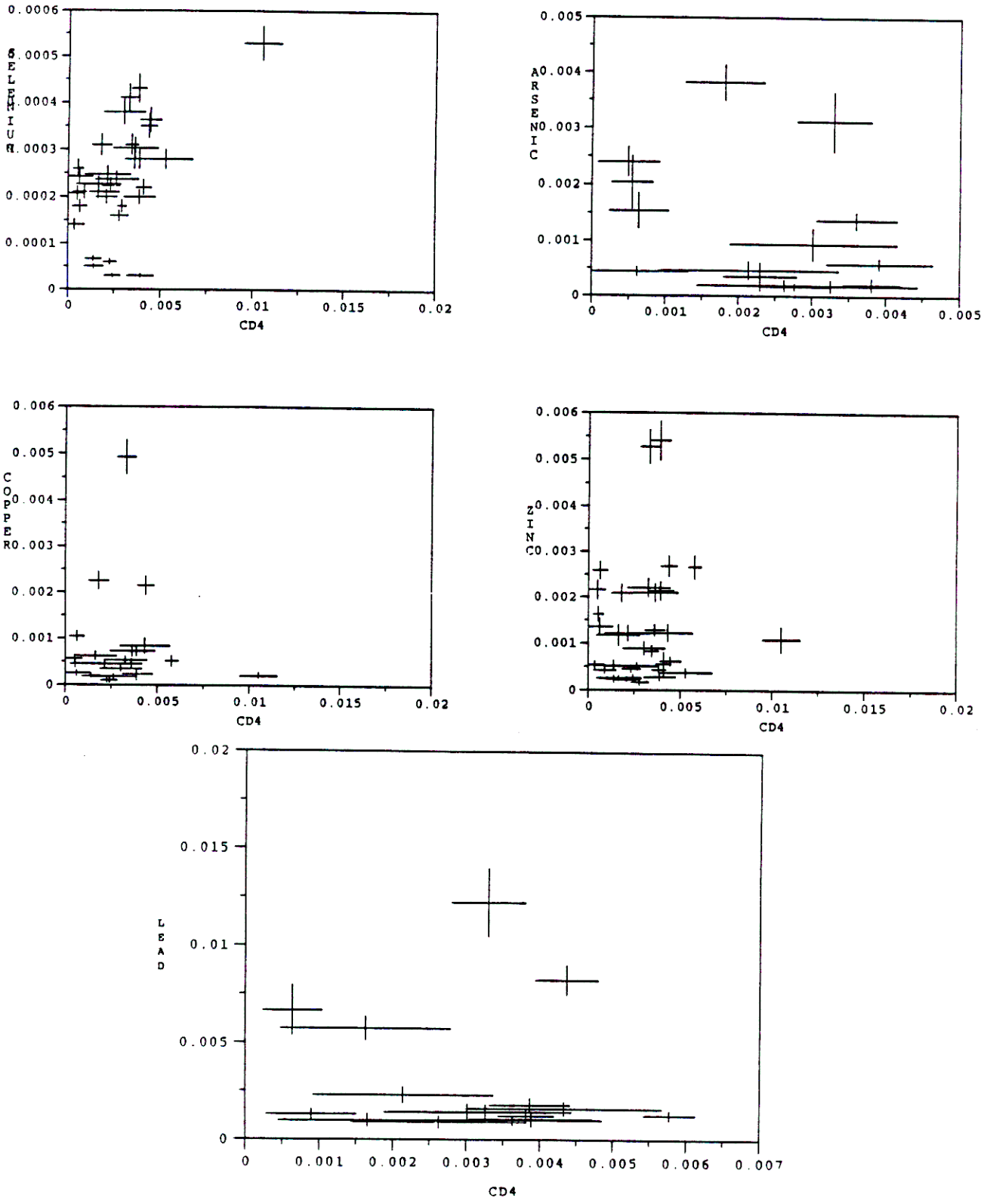

Figure 4.41: Scatter plots of fully scaled CD_4 (ppt) against the trace elements selenium, arsenic, copper, zinc, and lead ($\mu g/m^3$) at Hopi Point.

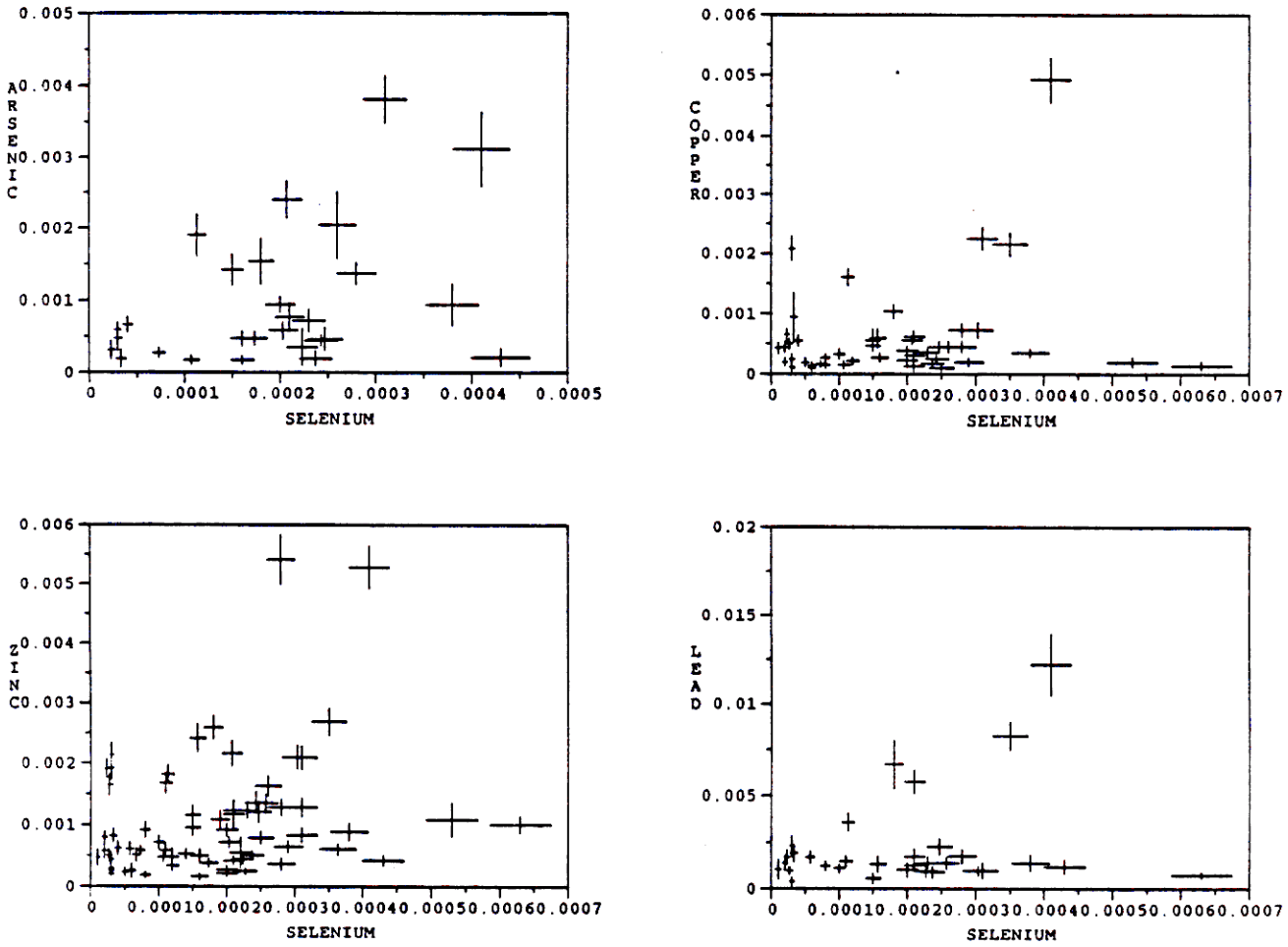

Figure 4.42: Scatter plots of the trace element selenium ($\mu g/m^3$) against the trace elements arsenic, copper, zinc, and lead ($\mu g/m^3$) at Hopi Point.

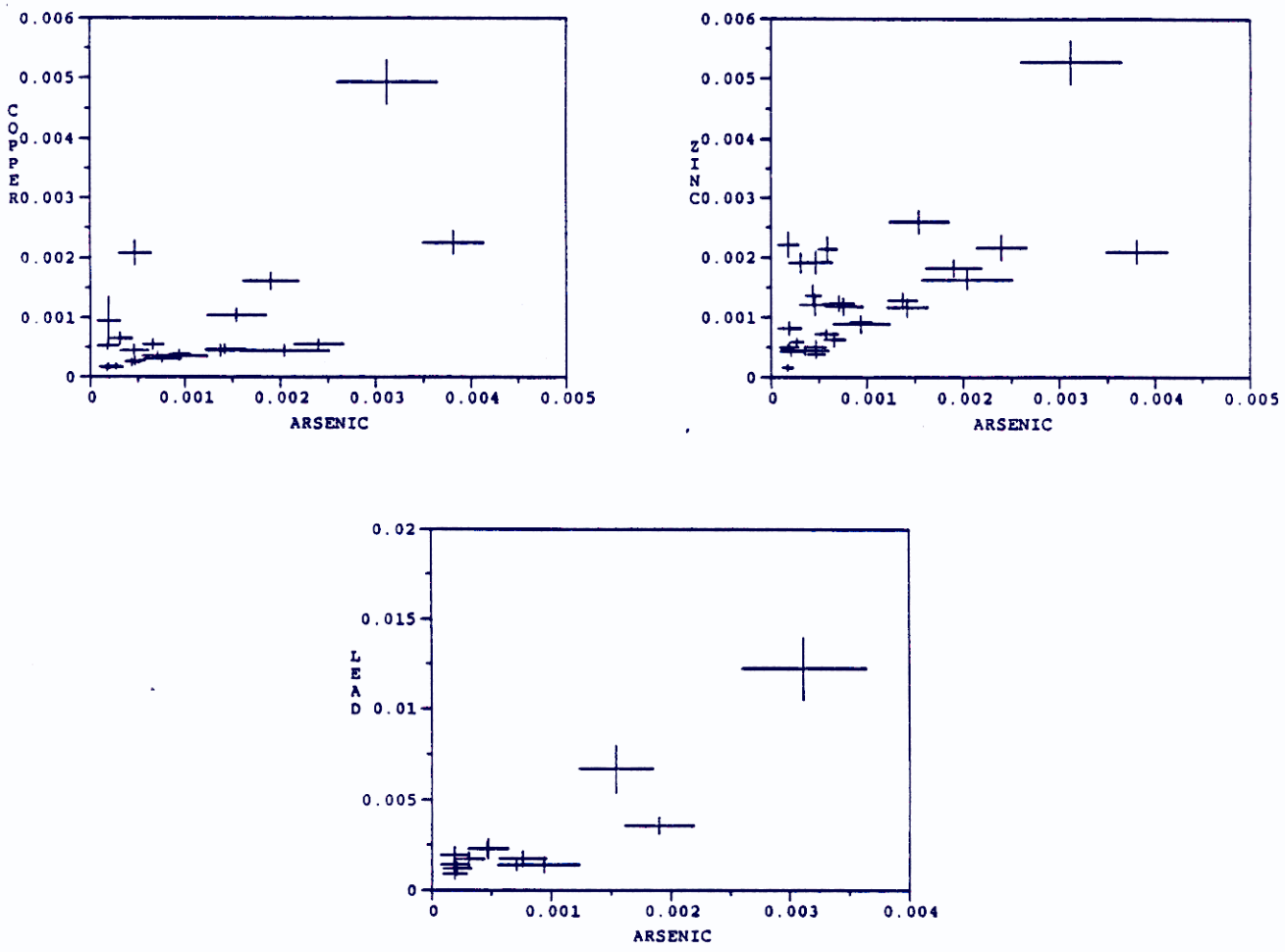

Figure 4.43: Scatter plots of the trace element arsenic ($\mu g/m^3$) against the trace elements copper, zinc, and lead ($\mu g/m^3$) at Hopi Point.

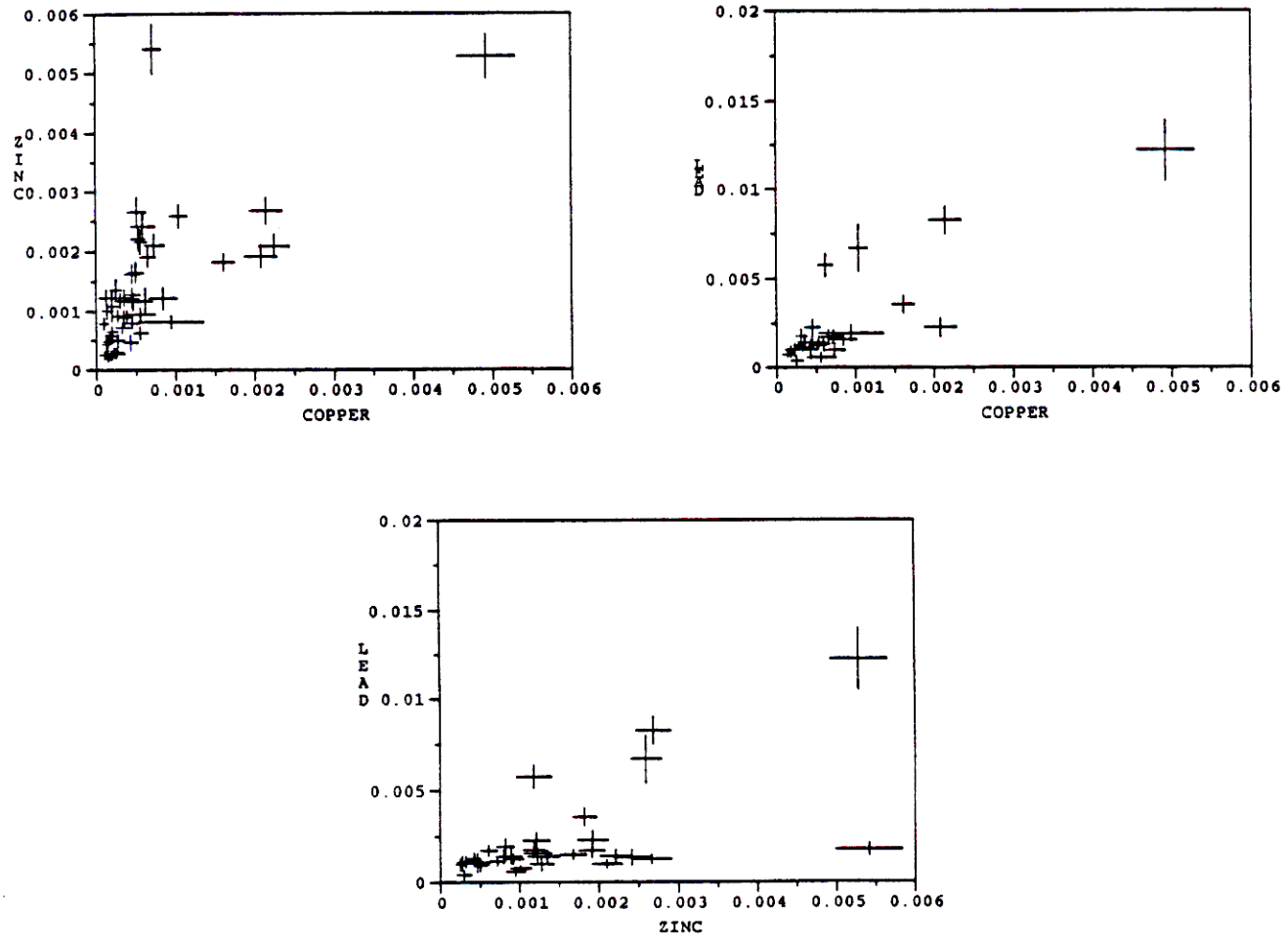

Figure 4.44: Scatter plots of the trace element copper ($\mu g/m^3$) against the trace elements zinc and lead ($\mu g/m^3$), and the scatter plot of the trace elements zinc and lead, at Hopi Point.